Air Qual Atmos Health (2016) 9:775–783
DOI 10.1007/s11869-015-0379-7

Investigating ozone episodes in Portugal: a wavelet-based approach

A. Monteiro[1] · S. Gouveia[2] · M.G. Scotto[3] · J. Lopes[1] · C. Gama[1] · M. Feliciano[4] · A.I. Miranda[1]

Received: 27 July 2015 / Accepted: 9 November 2015 / Published online: 20 November 2015
© Springer Science+Business Media Dordrecht 2015

Abstract During the summer season, ozone concentrations regularly exceed the legislation limits in the North of Portugal, namely at Douro Norte monitoring station. The origin of such ozone episodes has been widely reported in several studies although uncertainties regarding its origin still remain. This work intends to investigate how the ozone concentrations measured at the Douro Norte nearest stations, located at west and east directions, are related to those measured at Douro Norte by means of coherence and phase transformations methods. The episodes were selected according to the magnitude of the hourly ozone peaks and the occurrence of exceedances of the threshold value at least in two sites. The results point out that 60 % of the selected episodes highlight significant dependence between Douro Norte station and the other two monitoring sites, with different phase signal and a delay range from 2 to 4 h.

Keywords Monitoring stations · North Portugal · Ozone episodes · Wavelet transformation

✉ Alexandra Monteiro
alexandra.monteiro@ua.pt

[1] CESAM, Department of Environment and Planning, University of Aveiro, Aveiro, Portugal

[2] Institute of Electronics and Telematics Engineering of Aveiro (IEETA) and CIDMA, University of Aveiro, Averio, Portugal

[3] CEMAT and Instituto Superior Técnico, University of Lisbon, Lisboa, Portugal

[4] CIMO, Polytechnic Institute of Bragança, Braganca, Portugal

Introduction

Tropospheric ozone (O_3) is a well-known secondary photochemical pollutant of major importance possessing detrimental effects on health, natural/urban ecosystems, and materials (Brauer and Brook 1997; Hogsett et al. 1997; Ozen et al. 2002; Szyszkowicz et al. 2010; Roger et al. 2013). Photochemical pollution episodes in several European regions have been registered not only in urban/suburban sites but also in rural areas (Donev et al. 2002; Dueñas et al. 2004). This is the case of Douro Norte (DN), a rural air quality monitoring station located at an altitude of 1086 m in the Alvão Natural Park, in the northeast of Portugal, where ozone exceedances occur on a regular basis (Gouveia and Liberato 2008 ; Evtyugina et al. 2009; Carvalho et al. 2010). The high O_3 concentrations monitored at this station represent, on average, 30 % of the total alert threshold exceedances observed at the national monitoring network, reaching in 2005 more than 40 % (and more than 80 % of the information threshold exceedances). The annual average ozone concentration at this site is higher than 90 μg m^{-3}. This value is particularly high when compared to the average levels detected over the mid-latitudes of the Northern Hemisphere (40–90 μg m^{-3}) (Vingarzan 2004; Reid et al. 2008).

The geographic location, elevation, and extent of anthropogenic influence may contribute to the ozone levels variability. Regarding the high-altitude sites, it is often claimed that they are “above the boundary layer” or “representative of the free troposphere” by sole consideration of their elevation (Chevalier et al. 2007). However, mountains appear to considerably enhance atmospheric turbulence and affect circulation for many reasons (roughness, synoptic lifting, hydraulic effects, thermally induced circulations, etc), and thus, it can be hardly stated that even a high-altitude station is free from the influence of the surface without further investigation (Lefhon 1992; Sanz and Millán 2000).

Apart from this influence, the occurrence of ozone episodes can be related to two main sources, namely, the local scale production and the regional scale transport from other polluted regions (Borrego et al. 2002, 2003; Monteiro et al. 2005). Previous studies point out the role of the long-range transport on the ozone levels observed at DN site. Gama et al. (2009) studied the connection between the backward air mass trajectories and the ozone levels measured at this site between 2005 and 2007. The results show a significant influence of the transport path on ozone concentrations, which is more noticeable when the probability of occurring photochemical pollution phenomena is higher (summer), highlighting the role of photochemical production along long-range transport phenomena, and the input of pollutants into air masses, along their path. Monteiro et al. (2012) studied a high ozone episode which occurred in DN in July 2005 concluding that the ozone peaks observed at DN were not produced locally but as a result of transport phenomena. The importance of the long-range transport to the volatile organic compounds (VOC) ozone precursors in this specific rural mountain area is also discussed by Evtyugina et al. (2009). Carvalho et al. (2010) analysed a composite of days between 2004 and 2007 including the highest hourly ozone concentrations. The ozone-rich episodes at DN are in general connected with a positive temperature anomaly above the Iberian Peninsula and with a wind flow pattern from NE (which is the dominant pattern over the North of Portugal during the summer period), leading to an enhancement of the photochemical production and to the transport of pollutants from Spain to Portugal.

In this paper, we examine the connection between the O_3 time series simultaneously measured at DN and the two nearest monitoring stations to investigate the origin and formation of five ozone episodes during the period 2006–2013. Since O_3 time series are of non-stationary nature with substantial temporal changes in periodicities of environmental interest (e.g., daily period and others), the links between stations were explored by wavelet transforms (WT). In particular, wavelet coherence and phase were used to clarify the strength of the connection and the phase relationship of two monitoring stations at different time scales. Special attention was given to the time frequency regions exhibiting large coherence and a consistent phase relationship, thus, suggesting causality between the time series observed at different monitoring sites.

The rest of the paper is organized as follows: in Section "Ozone monitoring at North Portugal", the ozone concentration values measured at DN station and the two closest sites are presented and discussed. Section "Statiscal methods" describes the wavelet transformation method applied. Furthermore, the results are presented, analysed, and discussed in detail. Finally, in Section "Results and discussion", the main conclusions are summarized.

Ozone monitoring at North Portugal

In order to investigate the origin of the ozone measured at DN station, the ozone measured at the two nearest monitoring sites—Minho Lima (ML) and Instituto Politécnico Bragança (IPB)—were also compiled and analysed. The monitoring stations and O_3 data are described and the most relevant O_3 episodes selected to further (statistical) analysis.

Exploring the monitoring data set

Figure 1 indicates the location of the rural background station DN and the two nearest monitoring stations (ML and IPB). ML station is located westerly and is a station belonging to the Portuguese Air Quality Network (see http://qualar.apambiente.pt/) classified as rural background. IPB station, located at the east of DN, belongs to the Instituto Politécnico de Bragança, classified as background environment with urban influence since is located at Bragança city center.

The Air Quality Directive (Directive 2008/50/EC) establishes objectives for ambient air quality designed to avoid, prevent, or reduce harmful effects on human health and the environment as a whole. For ozone, information and alert thresholds are defined as well as target values for the protection of the human health and for the protection of vegetation. The target value for the protection of human health, 120 μg m^{-3}, is defined for the maximum daily 8-h mean concentration, selected by examining 8-h running averages, and is calculated from hourly data and updated on a hourly basis. According to the Air Quality Directive, this target value for the protection of human health cannot be exceeded on more than 25 days per calendar year averaged over 3 years. Figure 2 depicts the maximum daily 8-h mean concentration for the three stations, between 2006 and 2013 (IPL only started measuring in 2006). Furthermore, Table 1 summarizes the exceedances of the target value per calendar year and per station. In DN station, the number of exceedances is clearly above 25 in every year, highlighting that the target value for the protection of human health is not being accomplished. In ML and IPB stations, the accomplishment depends on the year which is considered. Looking to the exceedances averaged over the last 3 years (2011–2013), the target value is not accomplished in none of the stations.

Figure 3 shows the monthly and the diurnal variability of the O_3 concentrations per average day and season.

Although maximum hourly ozone concentrations are recorded during the summer period (due to photochemical production), it is during April that the maximum monthly

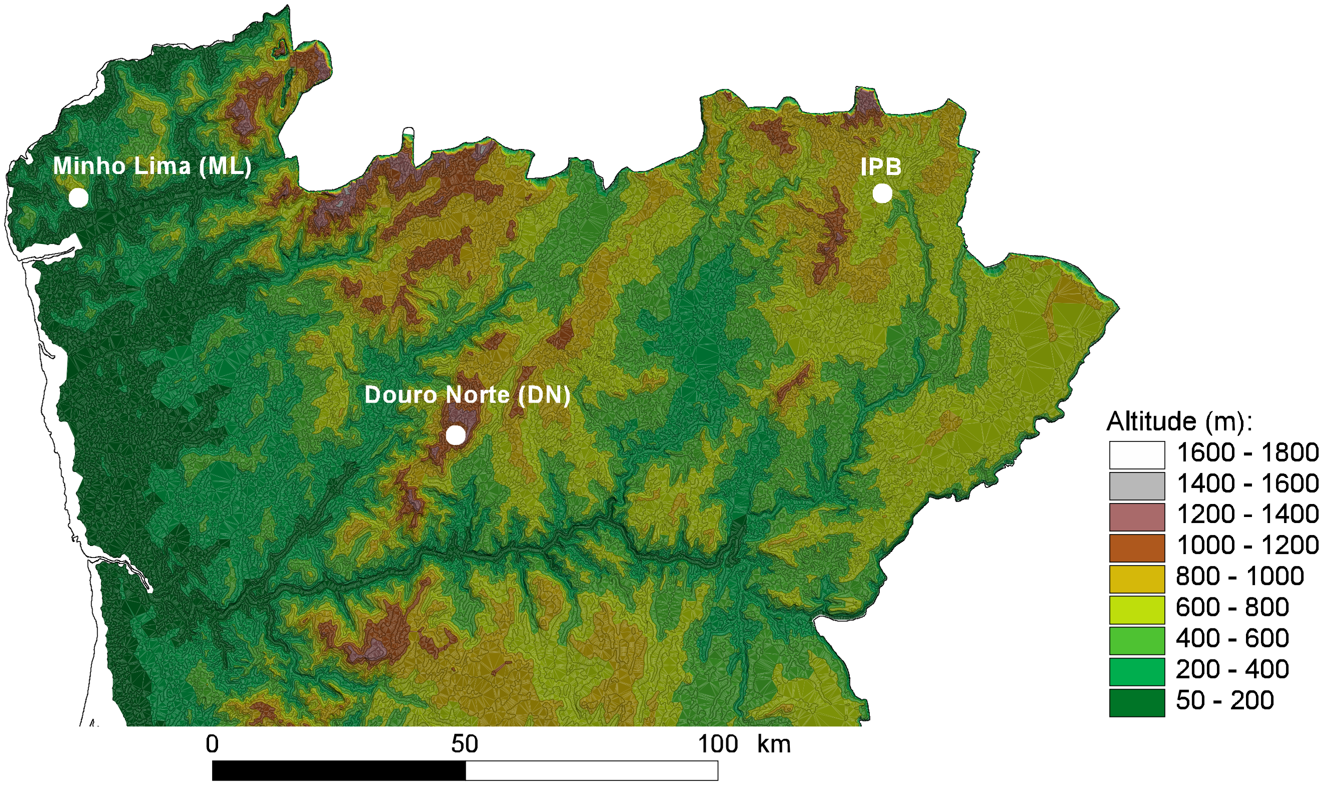

Fig. 1 Northeast of Portugal area and monitoring station locations and respective altitude

averaged concentrations are observed at the three sites (see Fig. 3). The spring ozone maximum is a characteristic of remote sites from the northern hemisphere. The state of the knowledge with respect to this maximum is synthesized by Monks (2000) who discusses the roles of stratospheric-tropospheric exchange and photochemistry, and considering the evidence for various mechanisms for accumulation of ozone and its precursors. During summer, ozone concentrations exhibit an obvious diurnal cycle at the three monitoring sites. In contrast, however, during the winter season, DN and ML sites exhibit a mean daily profile almost constant during the day, which is justified by the rural environment background influence. In IPB, ozone concentrations exhibit a diurnal cycle also during the winter, related to the

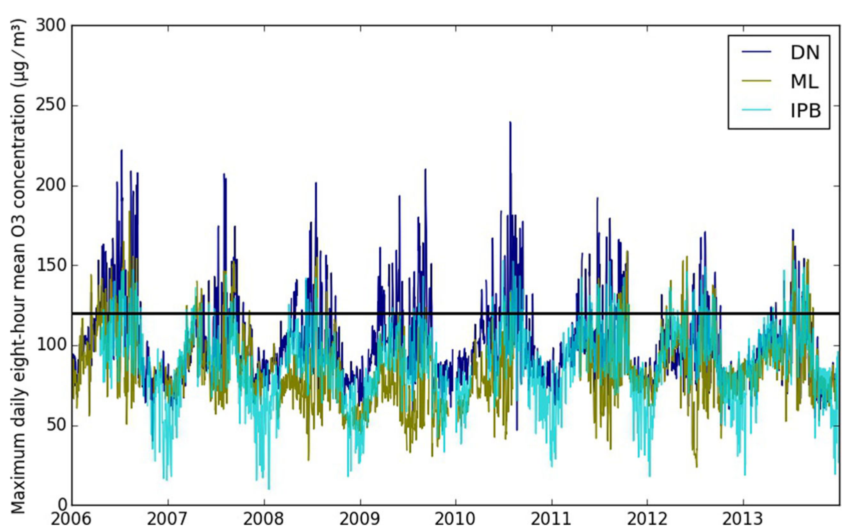

Fig. 2 Maximum daily 8-h mean ozone concentration measured at Douro Norte (DN), Minho-Lima (ML), and Instituto Politécnico de Bragança (IPB) for the period 2006–2013

Table 1 Number of exceedances to the target value for the protection of human health per calendar year

Year	DN	ML	IPB
2006	102	61	35
2007	45	37	19
2008	48	11	17
2009	77	1	7
2010	66	4	31
2011	67	28	47
2012	31	28	41
2013	36	35	41

urban influence and the presence of NOx emissions (and consequent titration of O_3 during night).

Episodes selection

In order to identify the most relevant ozone episodes in the area of study, data were filtered according to specific criteria, namely, (i) days exhibiting maximum daily 8-h mean ozone concentration higher than 120 μg m^{-3} and (ii) exceedances of the hourly information threshold 180 μg m^{-3} in at least two sites. Five case studies were selected. It is worth mentioning that because of the high O_3 values observed in this region these legal thresholds were chosen as criteria, nevertheless, other episodes could be identified if other thresholds had been considered (Saavedra et al. 2012). The evolution of the hourly ozone concentrations observed in the three sites during the 2-day case studies is presented in Fig. 4.

To better characterize the selected ozone episodes, 3-day back trajectories arriving at different altitude levels (100, 500, and 1000 m agl) at the three sites were calculated using the Hybrid Single-Particle Lagrangian Integrated Trajectory model (HYSPLIT, version 4.8) developed by the National Oceanic and Atmospheric Administration (NOAA)'s Air Resources Laboratory (ARL) (Draxler and Hess 2004) . The model uses gridded meteorological data from the NCAR-NCEP global reanalysis project. The resulted back air parcel trajectories for each of the episode days are depicted in Fig. 5.

The back trajectories analysis reveals similarities between the episodes, with air masses coming from North (Galiza and Castilla-Leon regions), with exception of episode 3, where a southern-east synoptic pattern is dominant. These specific synoptic conditions were already identified in a previous study Carvalho et al. (2010) as favorable for the occurrence of ozone episodes at DN site. The HYSPLIT back trajectories also show that some recirculation exist for episodes 1, 3, and 5.

Statistical methods

Wavelet-based analysis

Wavelet transform (WT) decomposition allows the computation of the coherence and the phase lag between two time series as a function of both time and frequency

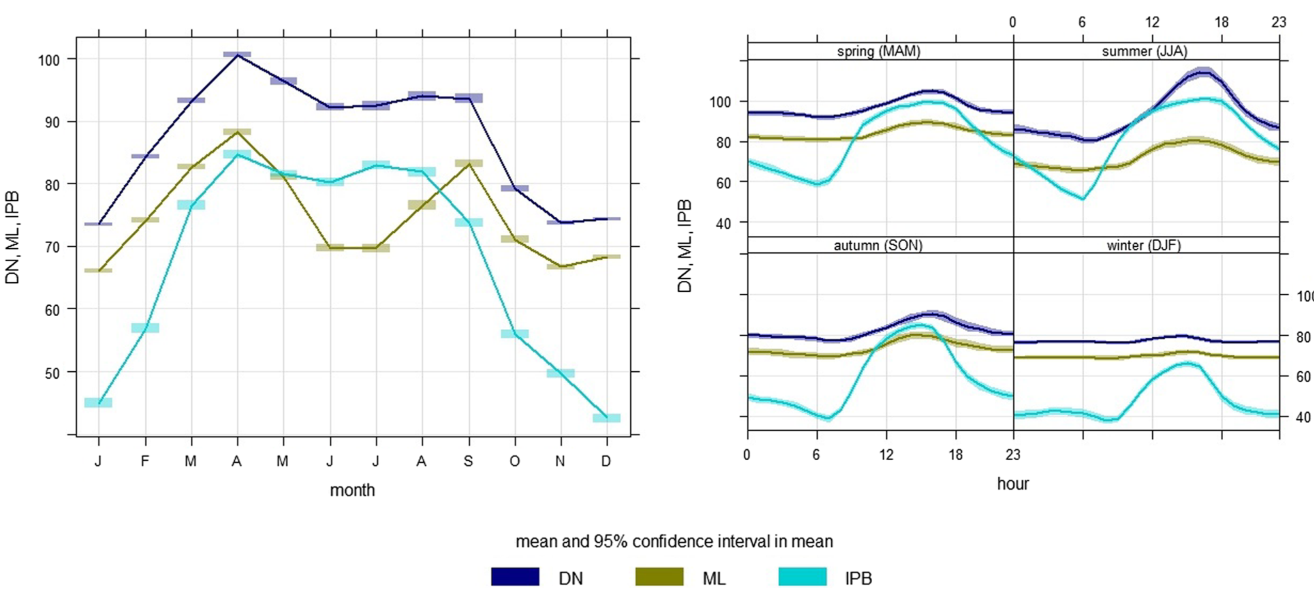

Fig. 3 Monthly and daily variability of the ozone concentrations at DN, ML, and IPB (considering the 2006–2013 period)

(Grinsted et al. 2004). Let (X, Y) be a pair of time series representing the input X_t and the output Y_t of a system defined for $t = 1, \ldots, T$. The cross-wavelet transform is defined as

$$W_{xy}(j,t) = W_x(j,t)W_y^*(j,t),$$

where $W_x(j,t)$ is the wavelet transform of X_t and $W_y^*(j,t)$ represents the complex conjugate of $W_y(j,t)$. The index $j = 1, 2, \ldots, J$, relates to the wavelet scale $\tau_j = 2^{j-1}$, which is associated with frequencies in the interval $[1/2^{j+1}, 1/2^j]$. Thus, τ_j-scale captures the joint dynamics of the series over intervals with duration from 2^j to 2^{j+1} time units. A comprehensive review of WT decomposition can be found in the book of Percival and Walden (2006) and the references therein.

Since $W_{xy}(j,t)$ is a complex function, it can be represented as the product

$$W_{xy}(j,t) = |W_{xy}(j,t)| \exp\{i \arg(W_{xy}(j,t))\},$$

where $|W_{xy}(j,t)|$ is the amplitude and $\arg(W_{xy}(j,t))$ is the complex argument. For independent processes X_t and Y_t, W_{xy} is null and thus one process is not capable of predicting the other. Likewise, large $|W_{xy}(j,t)|$ values indicate that X_t and Y_t exhibit strong linear dependence, at a given phase $\arg(W_{xy}(j,t))$. Thus, $|W_{xy}(j,t)|$ and $\arg(W_{xy}(j,t))$ functions should be interpreted together as WT analysis returns $\arg(W_{xy}(j,t))$ values as to maximize $|W_{xy}(j,t)|$ for each pair (j,t). As a consequence, the analysis of $\arg(W_{xy}(j,t))$ is merely suggestive of the causality between X_t and Y_t time series. In this formulation, phase allows the evaluation of lag τ such that $X_{t+\tau}$ and Y_t have highest covariance: $\tau < 0$ indicates that Y_t leads X_t whereas $\tau > 0$ indicates that X_t leads Y_t.

The X_t and Y_t covariance is also described in terms of the normalized squared modulus of $W_{xy}(j,t)$, i.e., the squared coherence, defined as

$$C_{xy}(j,t) := |W_{xy}(j,t)|^2 / W_x(j,t)W_y(j,t),$$

thus avoiding the need to define the range of "large" $|W_{xy}(j,t)|$ values. The real function $C_{xy}(j,t)$ varies between 0 and 1, where 1 indicates a perfect linear relationship between the two series at a given time t and a given frequency scale j. Therefore, $C_{xy}(j,t)$ can be used to quantify the strength of the time-frequency correlation between the two series in a normalized scale.

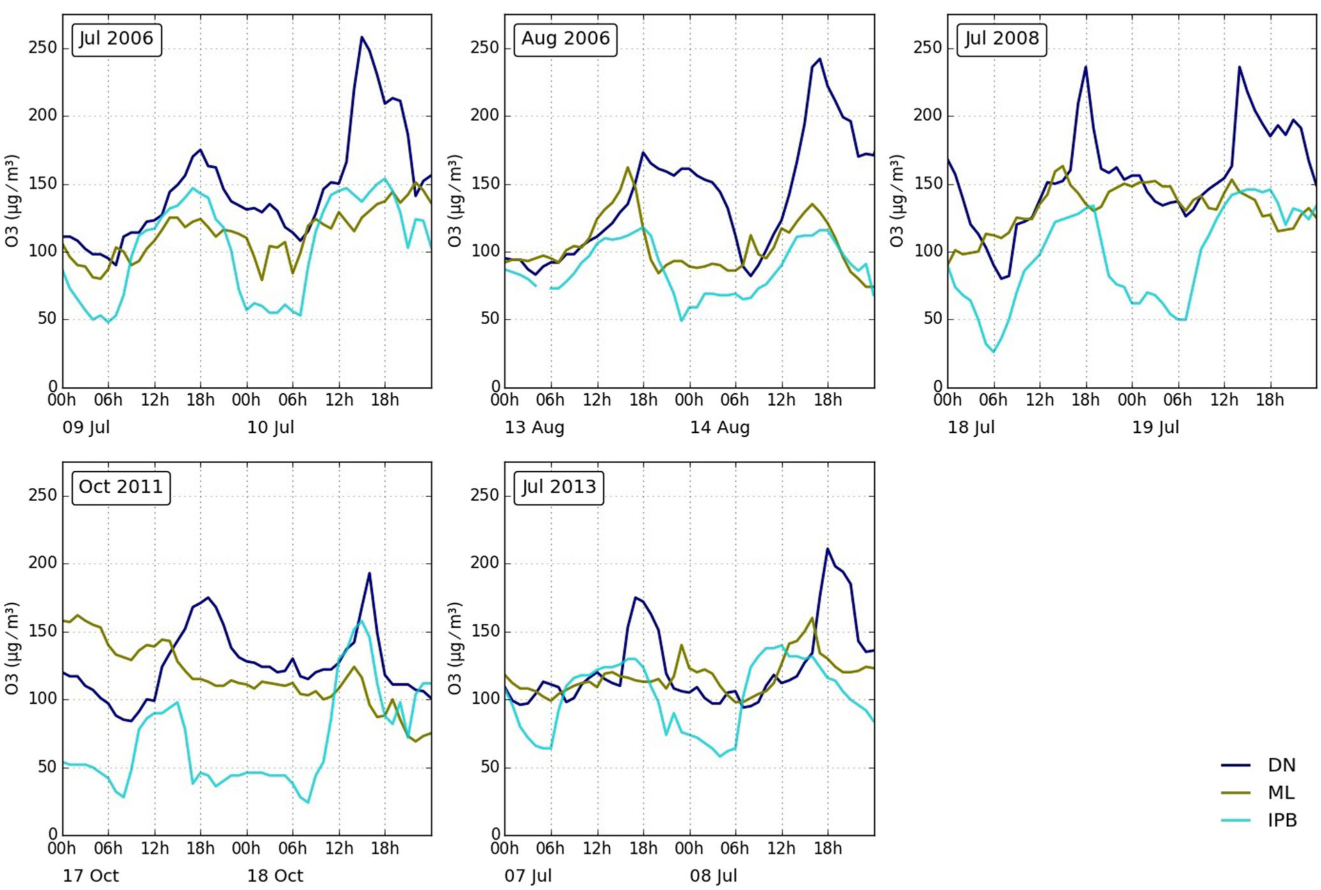

Fig. 4 Hourly mean ozone concentration measured at DN, ML, and IPB for the selected episodes

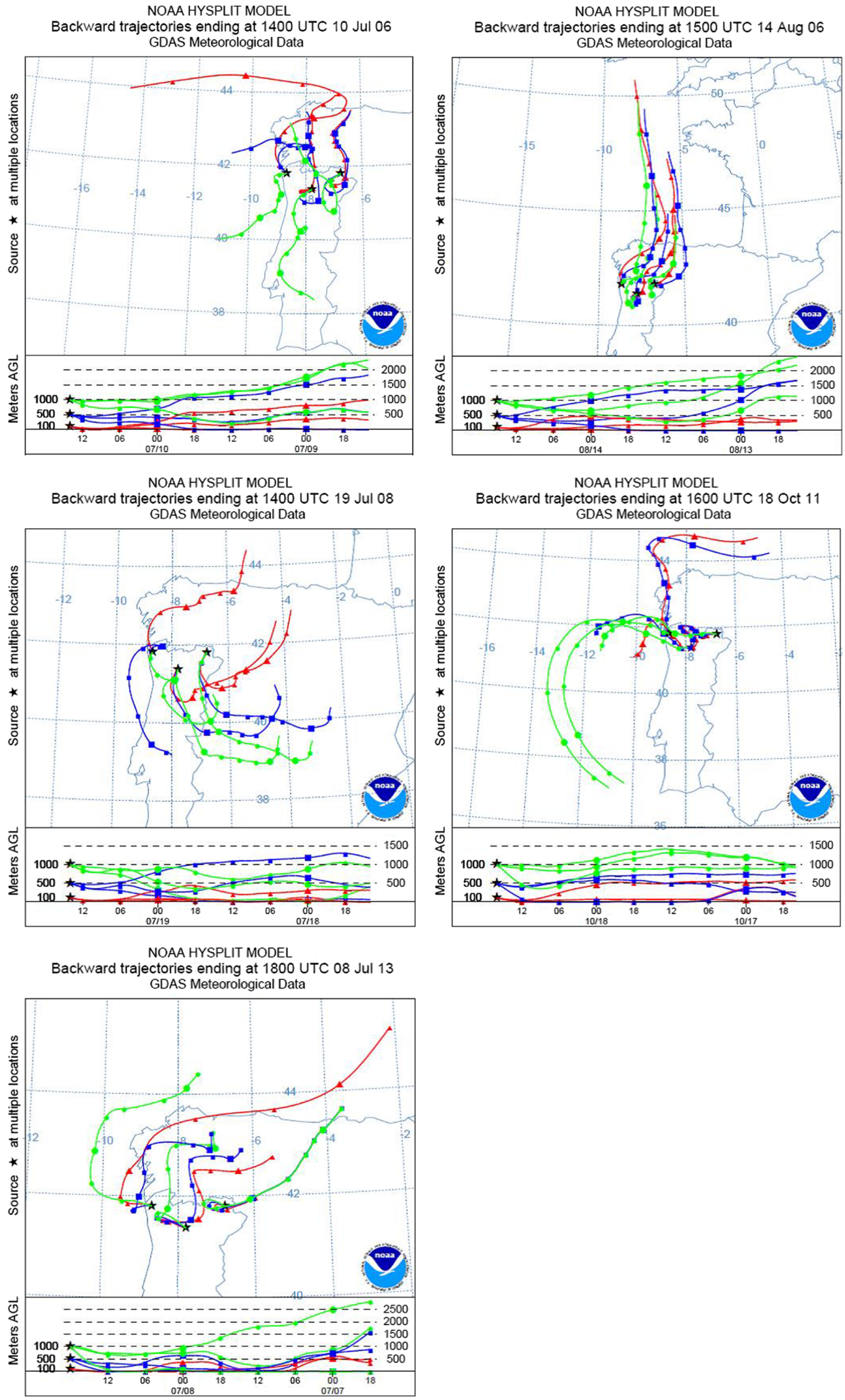

Fig. 5 Back trajectories for the selected episodes obtained with HYSPLIT model

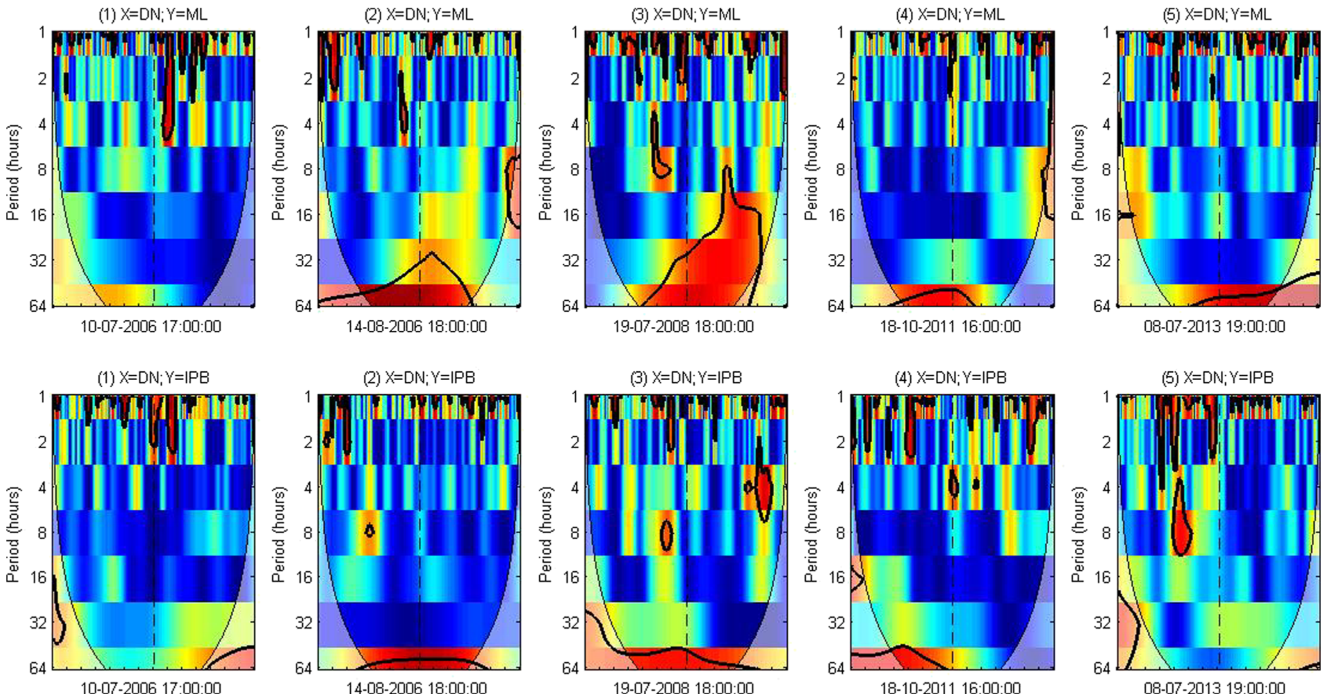

Fig. 6 Cross-wavelet transform of O_3 time series for DN − > ML (*top*) and for DN − > IPB (*bottom*) at the specified five episodes (columns). Temporal interval of analysis includes 7 days before and after the episode. The thick contour delimitates regions of significant coherence (at a 5 % level) and light shading shows regions influenced by edge effects

Squared coherence and phase were estimated using a Morlet wavelet with dimensionless frequency $\omega_0 = 6$, since it provides a good trade-off between time and frequency WT resolution (Grinsted et al. 2004). Furthermore, $J = 7$ was

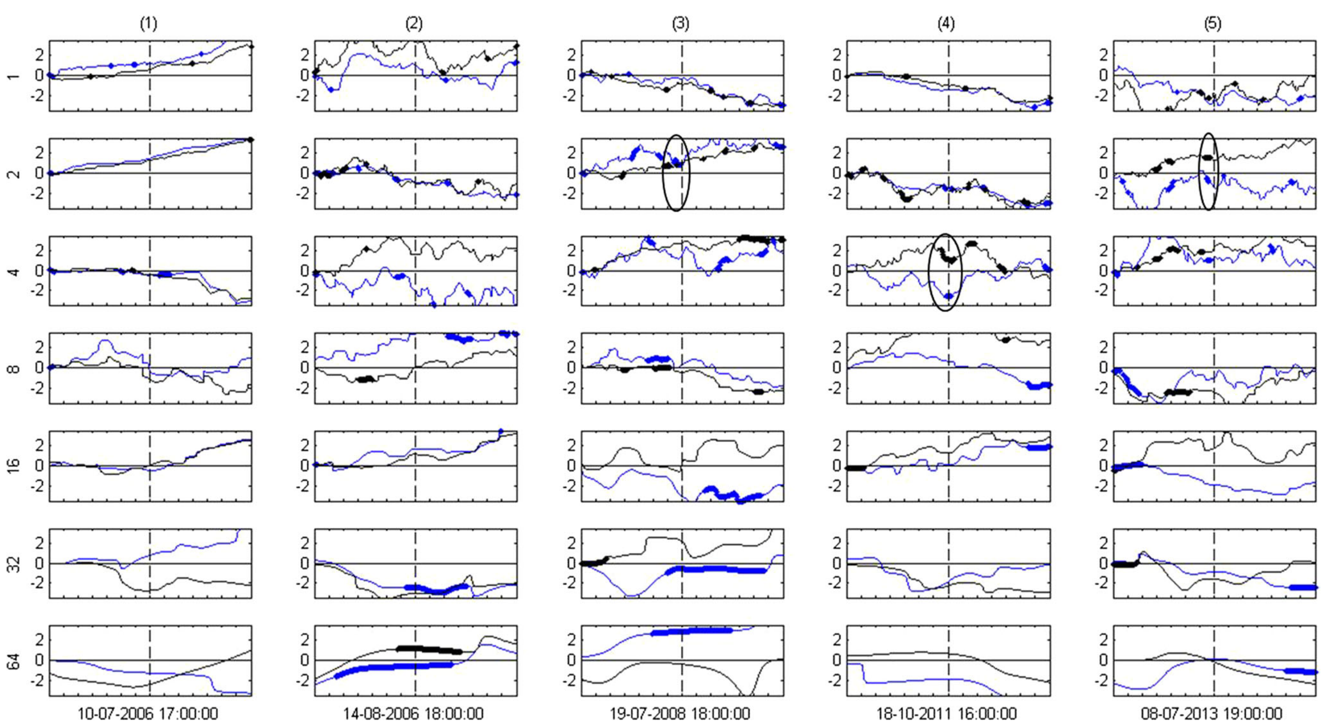

Fig. 7 Time-frequency analysis for the two time series (DN − > ML (*black*) and DN − > IPB (*blue*)) analysis and considering the time scale of 1, 2, 4, 8, 16, 32, and 64 h (*x*-axis) and a total of 6 days (7 days before the episode peak and 7 days after *y*-axis)

set to obtain the wavelet scales $\tau_j = 1, 2, 4, 8, 16, 32, 64$ thus including the intra-day ($j \leq 5$) and the daily periodicities ($j = 6$) in the WT analysis. The statistical significance of the coherence (and consequently the phase reliability) was assessed by simulation, described as follows (Torrence and Compo 1998; Grinsted et al. 2004): an ensemble of 300 surrogate series was generated from the original X_t and Y_t time series, being the wavelet coherence estimated for each pair of surrogates. The significance level was set as the 95 % of the surrogate coherence amplitudes, for each WT scale $j = 1, 2, \ldots, J$. Coherence values in the original series observed above this threshold were considered significant (at a 5 % level). Surrogate series were generated following a stationary first-order autoregressive process (AR(1)), which exhibits a power spectrum with decaying proportional to $1/f^2$ over the frequency range (i.e., red/brownian noise).

Results and discussion

Figure 6 shows the cross-wavelet transform of O_3 time series for the two series of data (DN − > ML and DN − > IPB) for the selected five episodes. Figure 7 presents also the time-frequency analysis for the two time series (DN − > ML and DN − > IPB) but for each time scale (of 1, 2, 4, 8, 16, 32, and 64 h) separately and with the signal of the phase highlighted. The temporal interval of analysis includes 7 days before and after the episode in order to have enough quantity of data to perform this cross-wavelet analysis and representation of large frequency domains.

As expected, high coherence (normalized co-variance) is found for time periods of 2–3 days (mainly for episodes 2, 3, and 5), which is related to the duration and prevalence of synoptic patterns, confirming the adequacy of this cross wavelet transform application. Regarding the smaller time periods, high correlation/coherence between the ozone time series is found for the episodes 3, 4, and 5 with distinct characteristics (phase signal and angle strength) and time period, as highlighted in the plot (black circles). In detail, we can concluded that

1. Episode 3: during this episode high coherence is found between DN − > IPB (positive angle) with a 2h-time lag;
2. Episode 4: in this episode high coherence is found for both time series—DN − > ML (positive angle) and IPB − > DN (negative angle)—with a time lag of about 4h;
3. Episode 5: high coherence found for ML − > DN (negative angle) with 2h-time lag.

For the other two episodes, no relevant correlation was observed for time periods/scales up to 16 h. This shows that the different ozone episodes studied in this work should have different origins. The episodes 1 and 2 have probably local influence or more important local sources, since no correlation was found with none of the other two neighbors monitoring sites (ML and IPB).

For the other three episodes, the high coherence signal found between at least two time series indicates some probable transport of ozone and its contribution to the peak concentration measured. Nevertheless, these three episodes (3, 4, and 5) have distinct characteristics, with different magnitude and angle phase (indicating the direction for the transport) and different time lags between the two ozone time series. This suggests that the ozone peaks measured at these three sites have different origins and explanations for the three episodes.

This statistical analysis is particularly important to investigate the causes and origins of the high concentrations of ozone measured in a particular place (as DN) in order to plan and establish efficient measures to reduce this pollutant concentration, in particular, to support the air quality plans that need to be developed for specific polluted areas (Borrego et al. 2015).

Conclusions

The high levels of ozone measured at DN station (North of Portugal) during pre-selected episodes were investigated by means of a cross-wavelet transformations of O_3 time series. This statistical technique allowed to evaluate the coherence (in both time and frequency domain) between the ozone values measured in DN and the two nearest monitoring sites, ML and IPB, located to the west and east of DN, respectively. The five episodes were selected according to the simultaneous occurrence of exceedances to the O_3 limit value in all the three stations and the magnitudes of the maximum daily value registered and are characterized in terms of O_3 daily profiles and origin of air masses (back trajectories). The results indicate that high coherence exist between two O_3 time series (ML/DN and DN/IPB) for three of the episodes (episodes 3, 4 , and 5), with different magnitude, angle phase, and time lag, which indicates some probable transport of ozone between the three different sites (with distinct directions along the three episodes). For the other two episodes (episodes 1 and 2), no relevant correlation was observed for time periods/scales inferior to 16 h, which suggest local influence on the ozone formation. These results pointed out that different conditions and origins are associated to the high ozone peaks measured at this particular rural site (DN) located at the north of Portugal clearly indicating that distinct mitigation measures have to be developed to reduce this pollutant concentration (with focus on local production and also on the long-term transport).

Acknowledgments The authors wish to thank the financial support of the Comissão de Coordenação e Desenvolvimento Regional do Norte (CCDR-N). Thanks are extended to the Portuguese Foundation for Science and Technology for the financial support through the Project MAPLIA (PTDC/AAG-MAA/4077/2012), and the PhD grant of Carla Gama (SFRH/BD/87468/2012) and the Pos-Doc grant of S. Gouveia (SFRH/-BPD/87037/2012), and CIDMA/UA project PEst-OE/MAT/UI4106/2014 (Centro de Investigação e Desenvolvimento em Matemática e Aplicações, CIDMA/UA, Aveiro, www.cidma.mat.ua.pt), and IEETA/UA project PEst-OE/EEI/-UI0127/2014 (Instituto de Engenharia Electrónica e Telemática de Aveiro, IEETA/UA, Aveiro, www.ieeta.pt).

References

Borrego C, Miranda AI, Coutinho M, Ferreira J, Carvalho AC (2002) Air quality management in Portugal: example of needs and available tools. Environ Pollut 120:115–123. doi:10.1016/S0269-7491(02)00134-3

Borrego C, Tchepel O, Costa AM, Amorim JH, Miranda AI (2003) Emission and dispersion modelling of Lisbon air quality at local scale. Atmos Environ 37:5197–5205. doi:10.1016/j.atmosenv.2003.09.004

Borrego C, Monteiro A, Martins H, Ferreira J, Fernandes AP, Rafael S, Miranda AI, Guevara M, Baldasano JM (2015) Air quality plan for ozone: an urgent need for North Portugal. Air Qual Atmos Health. doi:10.1007/s11869-015-0352-5. in press

Brauer M, Brook JR (1997) Ozone personal exposure and health effect for selected groups residing in the Fraser Valley. Atmos Environ 31:113–121. doi:10.1016/S1352-2310(96)00129-X

Carvalho A, Monteiro A, Ribeiro I, Tchepel O, Miranda AI, Borrego C, Saavedra S, Souto JA, Casares JJ (2010) High ozone levels in the Northeast of Portugal: analysis and characterization. Atmos Environ 44:1020–1031. doi:10.1016/j.atmosenv.2009.12.020

Chevalier A, Gheusi F, Delmas R, Ordoñez C, Sarrat C, Zbinden R, Thouret V, Athier G, Cousin JM (2007) Influence of altitude on ozone levels and variability in the lower troposphere: a ground-based study for Western Europe over the period 2001–2004. Atmos Chem Phys 7:4311–4326. doi:10.5194/acp-7-4311-2007

Donev E, Zeller K, Avramov A (2002) Preliminary background ozone concentrations in the mountain and coastal areas of Bulgaria. Environ Pollut 117:281–286. doi:10.1016/S0269-7491(01)00192-0

Draxler RR, Hess GD (2004) Description of the HYSPLIT 4 modelling system. Techinal Memorandum ERL ARL-224. NOAA Air Resources Laboratory, Silver Spring, MD

Dueñas C, Fernández CM, Cañete S, Carretero J, Liger E (2004) Analyses of ozone in urban and rural sites in Málaga (Spain). Chemosphere 56:631–639. doi:10.1016/j.chemosphere.2004.04.013

Evtyugina MG, Nunes T, Alves C, Marques MC (2009) Photochemical pollution in a rural mountainous area in the Northeast of Portugal. Atmos Res 92:151–158. doi:10.1016/j.atmosres.2008.09.006

Gama C, Nunes T, Marques MC, Ferreira F (2009) Contribution of long-range transport to the ozone levels recorded in the Northeast of Portugal. Geophys Res Abstr 11, EGU2009-11256-1, Vienna, Austria

Gouveia C, Liberato MLR (2008) Local circulations over complex terrain in the Northeast of Portugal - Modelling O_3 transport. Geophys Res Abstr 10, EGU2008-A-09628, Vienna, Austria

Grinsted A, Moore JC, Jevrejeva S (2004) Application of the cross wavelet transform and wavelet coherence to geophysical time series. Nonlin Processes Geophys 11:561–566. doi:10.5194/npg-11-561-2004

Hogsett WE, Weber JE, Tingey D, Herstrom A, Lee EH, Laurence JA (1997) Environmental auditing: an approach for characterizing tropospheric ozone risk to forests. Environ Manage 21:105–120. doi:10.1007/s002679900010

Lefhon AS (1992) Surface level ozone exposures and their effects on vegetation. Lewis Publishers, USA

Monks P (2000) A review of the observations and origins of the spring ozone maximum. Atmos Environ 34:3545–3561. doi:10.1016/S1352-2310(00)00129-1

Monteiro A, Vautard R, Borrego C, Miranda AI (2005) Long-term simulations of photo oxidant pollution over Portugal using the CHIMERE model. Atmos. Environ 39:3089–3101. doi:10.1016/j.atmosenv.2005.01.045

Monteiro A, Strunk A, Carvalho A, Tchepel O, Miranda AI, Borrego C, Saavedra S, Rodríguez A, Souto J, Casares J, Friese E, Elbern H (2012) Investigating a high ozone episode in a rural mountain site. Environ Pollut 162:176–189. doi:10.1016/j.envpol.2011.11.008

Ozen BF, Mauer LJ, Floros ID (2002) Effects of ozone exposure on the structural, mechanical and barrier properties of select plastic packaging film. Packag Technol Sci 15:301–311. doi:10.1002/pts.602

Percival DB, Walden AT (2006) Wavelet methods for time series analysis. Cambridge University Press, Cambridge

Reid N, Yap D, Bloxam R (2008) The potential role of background ozone on current and emerging air issues: an overview. Air Qual Atmos Health 1:19–29. doi:10.1007/s11869-008-0005-z

Roger DP, Samoli E, Pham L, Dominici F, Touloumi G, Ramsay T, Burnett RT, Krewski D, Tertre AL et al (2013) Acute effects of ambient ozone on mortality in Europe and North America: results from the APHENA study. Air Qual Atmos Health 6:445–453. doi:10.1007/s11869-012-0180-9

Saavedra S, Rodríguez A, Taboada JJ, Souto JA, Casares JJ (2012) Synoptic patterns and air mass transport during ozone episodes. Sci Total Environ 441:97–110. doi:10.1016/j.scitotenv.2012.09.014

Sanz MJ, Millán MM (2000) Ozone in the Mediterranean region: evidence of injury to vegetation. In: Innes JL, Oleksyn J (eds) Proceedings of the Forest Dynamics in Heavily Polluted Regions. CAB International, pp 165–192

Szyszkowicz M, Porada E, Searles G, Rowe BH (2010) Ambient ozone and emergency department visits for skin conditions. Air Qual Atmos Health 5:303–309. doi:10.1007/s11869-010-0092-5

Torrence C, Compo GP (1998) A practical guide to wavelet analysis. Bull Am Meteorol Soc 79:61–78. doi:10.1175/1520-0477(1998)079<0061:APGTWA>2.0.CO;2

Vingarzan R (2004) A review of surface ozone background levels and trends. Atmos Environ 38:3431–3442. doi:10.1016/j.atmosenv.2004.03.030